

Copyright © 2002 IEEE

Reprinted from
IEEE Antenna's and Propagation Magazine, Vol. 44, No. 3, June 2002

This material is posted here with permission of the IEEE. Such permission of the IEEE does not in any way imply IEEE endorsement of any of Universität Ulm's products or services. Internal or personal use of this material is permitted. However, permission to reprint/republish this material for advertising or promotional purposes or for creating new collective works for resale or redistribution must be obtained from the IEEE by writing to pubs-permissions@ieee.org.

By choosing to view this document, you agree to all provisions of the copyright laws protecting it.

Millimeter-Wave Folded Reflector Antennas with High Gain, Low Loss, and Low Profile

Wolfgang Menzel¹, Dietmar Pilz², and Maysoun Al-Tikriti³

^{1,3}University of Ulm, Microwave Techniques
D-89081 Ulm, Germany

¹Tel: +49-731-5026350; Fax: +49-731-5026359; E-mail: wolfgang.menzel@ieee.org

³Tel: +49-731-5026356; Fax: +49-731-5026359; E-mail: maysoun@mwt.e-technik.uni-ulm.de

²EADS

D-89070 Ulm, Germany

Tel: +49-731-392-5855; E-mail: dietmar.pilz@vs.dasa.de

Abstract

Periodic and quasi-periodic structures, printed on a dielectric substrate, can be employed to control the reflection and transmission properties of incident waves as a function of structure geometry. Local variations of the element geometry on a substrate with backside metallization – resulting in respective variations of the reflection phase angle – can be used to design printed reflectarray antennas. The dual-polarization properties of such antennas, together with polarizing grids or slot arrays, can be exploited for the realization of compact, low-profile folded reflector antennas. Examples of some antennas of this type are presented, covering the 60 GHz range for communication and ISM applications, and 76 to 77 GHz for automotive radars.

Keywords: Millimeter-wave antennas; microstrip antennas; scanning antennas; multibeam antennas; reflectarrays; folded antennas; antenna arrays

1. Introduction

Antennas with low profile, low loss, and low production cost are of increasing importance for communication and sensor applications. While planar antennas are optimum with respect to antenna depth and cost, they suffer from high losses, especially for narrow beamwidths. Arrays of horn antennas, with a waveguide-feed network or waveguide slotted arrays, are lower in loss, but are somewhat complicated in their design, and they do not readily lend themselves to low-cost fabrication. As an alternative solution for printed low-cost antennas, this contribution describes quasi-optically fed printed and folded reflector antennas. These are printed reflectarrays, consisting of arrays of printed patches acting as fixed-reflection phase shifters and a printed polarization diplexer, e.g., a printed grid or slot array.

The basis for the design of the planar reflector is a periodic array of patches, printed on a dielectric substrate with backside metallization. With a plane wave incident from broadside, the complete power is reflected. The phase angle, however, depends on patch length and, to a minor degree only, on patch width (Figure 1). The reflection behavior of this arrangement is calculated using a spectral-domain method, e.g. [1]. The phase angle varies over nearly 360°. Thus, such elements can be used as reflection phase shifters. The phase angles calculated from a periodic structure can even be used for the design of the reflecting elements in planar reflector antennas, with the patches on a periodic grid, but with varying dimensions [2-5].

It should be noted that the reflection phase angle is adjusted by the dimensions of the patches themselves, these mostly being far from resonance. Consequently, in contrast to arrays based on microstrip half-wavelength *resonant* patches, with additional transmission lines for phase adjustment [6], the reflectarrays employed in this work exhibit quite low losses. By making use of an *independent* choice of lengths and widths of the printed patches, different properties for the two polarizations can be realized, i.e., dual-function or dual-frequency antennas [4, 7]. The focusing array can be modified to include a *polarization twisting* of the electromagnetic field, which, together with a printed polarizing grid or a slot array, leads to a folded reflector antenna [7-9].

For the antennas presented here, the patches are arranged on a quadratic grid. Consequently, the reflection phase angle for the orthogonal polarization can be read from Figure 1 by simply interchanging the length and width of a patch. This is indicated in Figure 1 by the two dots, representing an element 1.6 mm and 1.3 mm in size. The phase angle for an *E* field parallel to the longer axis (1.6 mm length) of the element is approximately 70°, and the reflection phase angle is about -110° for the orthogonal polarization, i.e., a phase difference of 180° between the two polarizations.

2. Basic Principle and Design of the Folded Reflector Antennas

The principal function of a printed folded reflector antenna is indicated in Figure 2. The antenna consists of a feed, a planar

polarization filter, and a printed reflectarray. The feed is typically a cylindrical-waveguide feed horn, but a planar structure may equally be used. The polarization filter may be a grid or a resonant slot array, printed on a dielectric substrate, acting, at the same time, as a radome. The polarizing grid or slot array is designed using a standard mode-matching procedure, including metallization thickness. Either of these polarizers reflects one polarization, and is transparent for the other polarization.

The radiation from the feed is polarized in such a way that it is reflected by the printed grid or slot array at the front of the

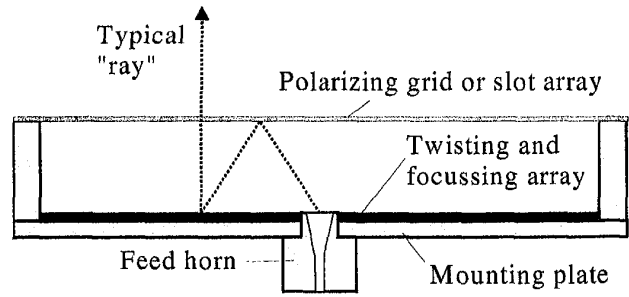


Figure 2. The basic principle of the folded reflector antenna.

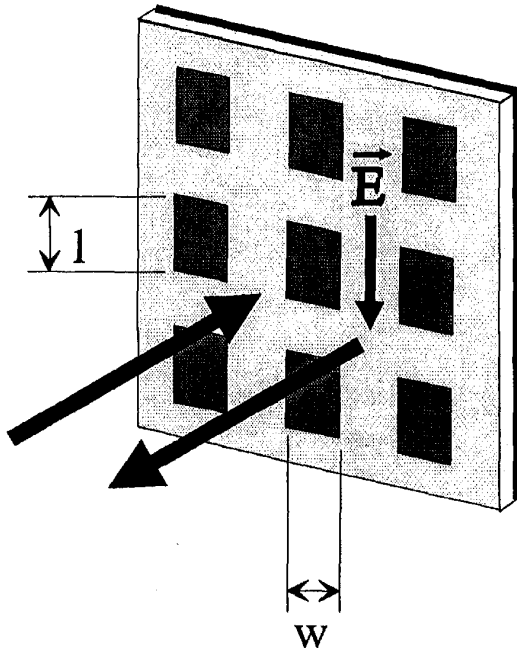


Figure 1a. A periodic array of patches.

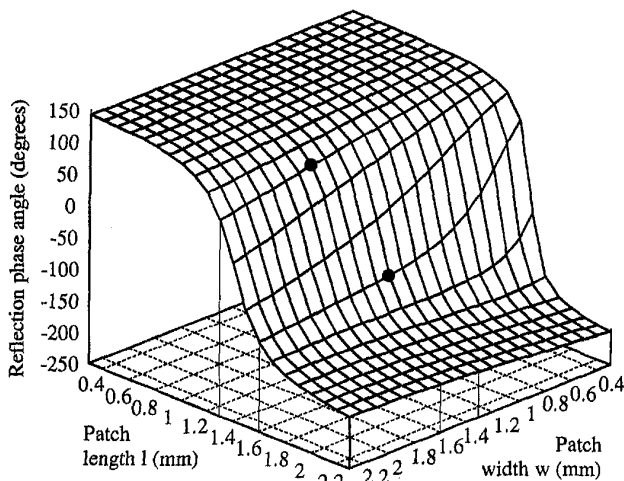


Figure 1b. The reflection phase angle as a function of the patch geometry for the array in Figure 1a (substrate thickness: 0.254 mm, dielectric constant: 2.22, element distances: 2.4 mm \times 2.4 mm, frequency: 60 GHz). The two dots indicate two examples of phase angles for patches of 1.3 mm \times 1.6 mm and 1.6 mm \times 1.3 mm, respectively.

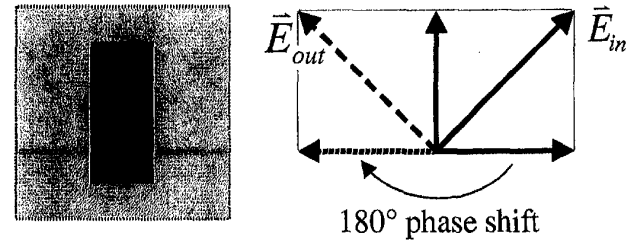


Figure 3. A single cell/patch, and the vector decomposition of the incident and reflected electric field for 180° of reflection phase-angle difference.

antenna (Figure 2). Then, the wave is incident on the reflectarray with the printed patches. This reflectarray is the key component of the antennas reported on in this paper. The patch axes of this array are tilted by 45° with respect to the incident electric field. The electric-field vector can be decomposed into the two components parallel to the patch axes (Figure 3), and the reflection properties can be determined separately. The dimensions of the patches are selected in such a way that a phase difference of 180° occurs between the reflection phase angles of these two components. An example of such a patch, with a length of 1.6 mm and a width of 1.3 mm, is indicated in Figure 1: the two dots represent the behavior of this element for the two orthogonal polarizations. Superposition of the reflected field components then leads to a twisting of the polarization by 90° (Figure 3). The necessary 180° phase-angle difference between the two field components of the reflected wave can be achieved for a large number of combinations of length and width of the patches, differing by their *absolute* reflection phase angle. This degree of freedom is now used to adjust the required phase angles, to transform the incident spherical wave into an outgoing plane wave. To this end, ray tracing is employed, together with the condition of an equal phase front of the outgoing wave. This plane wave, with twisted polarization, can then pass through the grid or slot array.

As already indicated above, the design of the reflectarray is done simply on the basis of *periodic* arrays of patches, and a *normal incidence* of a plane wave. The reflection phase angles are calculated in steps of 0.01 mm of the element dimensions, similarly to what is plotted in Figure 1. The optimum combination of reflection phase angles for the two polarizations is then selected from this set of data, according to both twisting and focusing requirements. Although this design procedure includes several approximations, it has proven successful, as can be seen from the results given in the following sections.

3. Results

3.1 Single-Beam Antennas

Several printed folded reflector antennas, as shown in principle in Figure 2, have been designed, fabricated, and tested. Figure 4 displays the layout of a printed reflector of a V-band antenna with a circular aperture. The diameter of this antenna was 100 mm. The distance between reflector and polarizer was 25 mm, resulting in a focal length of 50 mm, or an f/D of 0.5. The reflectarray and the polarizing grid of this antenna were printed on 0.254 mm and 1.58 mm thick Duroid, respectively. The dielectric constants were 2.2 and 2.5. As a feed element, a circular waveguide horn, with an aperture diameter of 5.5 mm, was used.

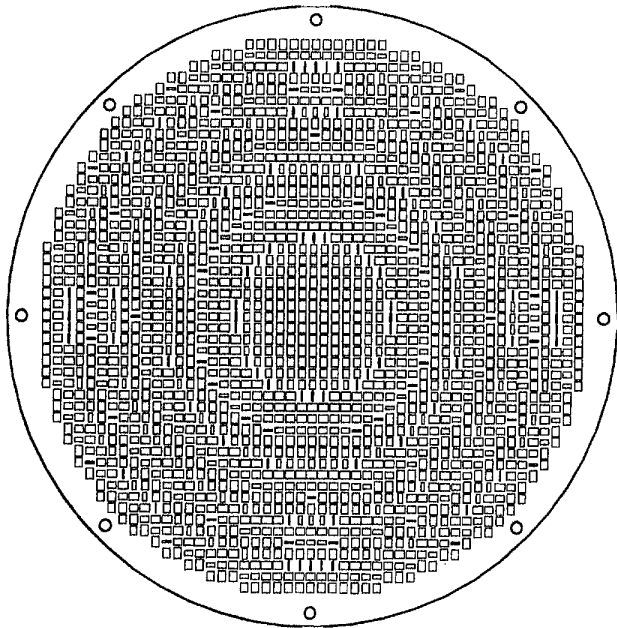


Figure 4. The layout of a V-band reflectarray for a folded reflector antenna.

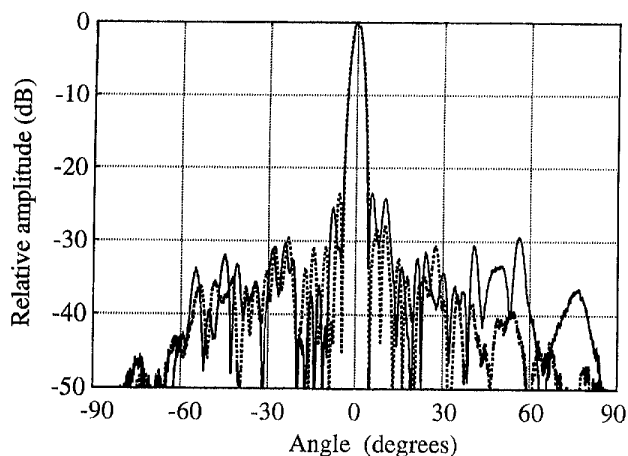


Figure 5. The E -plane (solid line) and H -plane (dotted line) radiation diagrams of the V-band folded reflector antenna (frequency: 61 GHz, diameter: 100 mm, antenna height: 25 mm.)

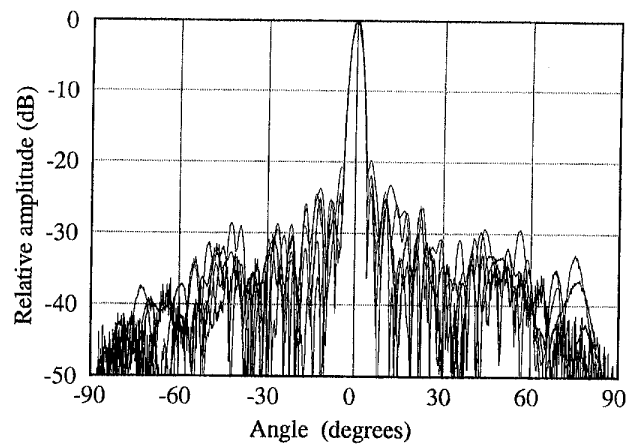


Figure 6. The E -plane radiation diagrams of the V-band folded reflector antenna for different frequencies (58-62 GHz in 1 GHz steps).

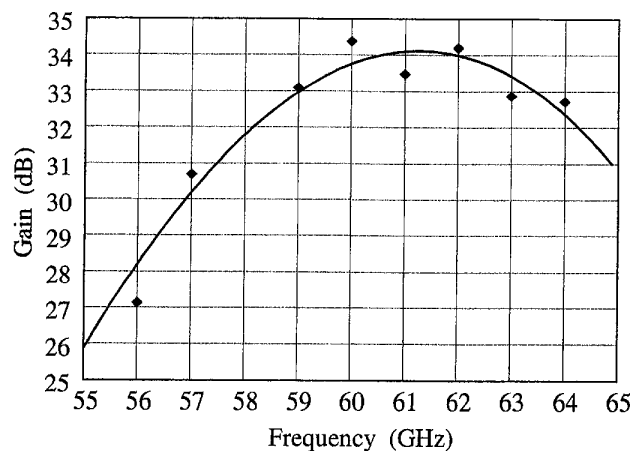


Figure 7. The gain of the V-band folded reflector antenna (25 mm depth). The dots represent measured values; the solid line is a least-squares polynomial approximation of the measured values.

In Figure 5, E - and H -plane radiation diagrams are plotted for this antenna, at the design frequency of 61 GHz. The beamwidths were 3.2° and 3.4° in the E and H planes, respectively. The sidelobe level was better than -24 dB. E -plane radiation diagrams at different frequencies are given in Figure 6, showing nearly the same beamwidths and a sidelobe level better than -20 dB between 58 GHz and 62 GHz. A similar performance over frequency has been achieved for the H plane. The antenna gain has been measured between 55 GHz and 64 GHz (Figure 7). The maximum gain was 34 dB, and a bandwidth of about 7 GHz for a 3 dB reduction of gain can be stated.

To further reduce the antenna depth, tests were made with a closer distance between reflector and polarizer, thus reducing the focal length of the reflectarray. Figure 8 displays the radiation patterns of an antenna with a diameter of 100 mm and only 15 mm in depth. Again, a reasonably good radiation performance was shown. The far-off sidelobe level in the H plane was slightly increased, and the gain was reduced to 31.5 dB. This was due to increasing phase errors, resulting from the simplifying assumptions

for the design procedure, as described above. The angle of incidence of the feed radiation varied over a wider angle of incidence, and due to a faster change in the required reflection phase angles, a stronger variation in patch size occurred.

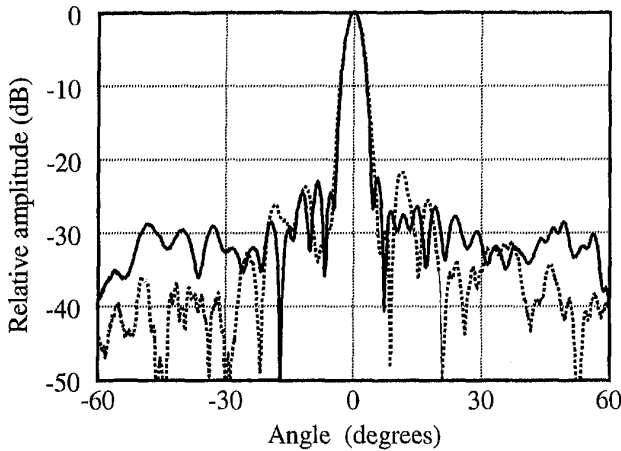


Figure 8. The *H*-plane (solid line) and *E*-plane (dotted line) radiation diagrams of a V-band folded reflector antenna with reduced height (frequency: 58 GHz, diameter: 100 mm, antenna height: 15 mm).

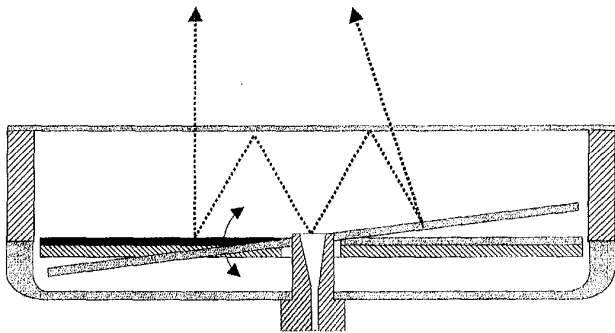


Figure 9. The principle of mechanical beam scanning with the folded reflector antenna.

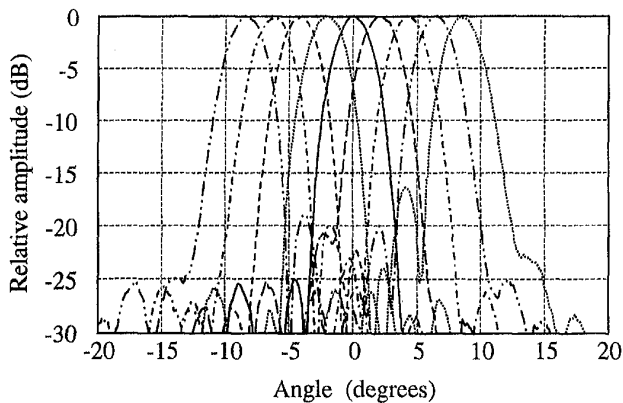


Figure 10. The *H*-plane radiation diagrams of the mechanically scanned antenna (scanning in the *H* plane, antenna diameter: 100 mm, antenna depth: 25 mm, frequency: 76.5 GHz).

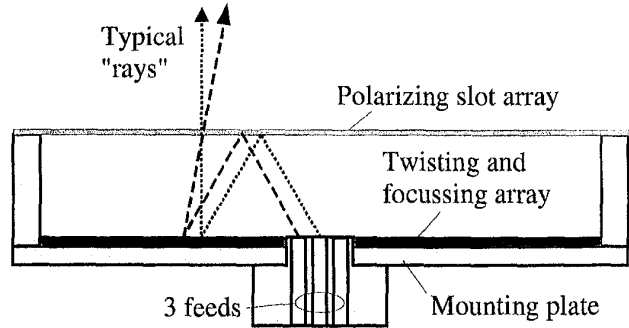


Figure 11. The principle of a folded reflector antenna with beam scanning using multiple feeds.

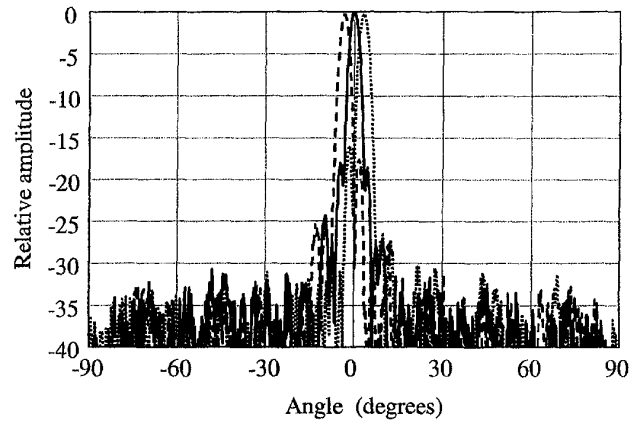


Figure 12a. The overall *E*-plane radiation diagram of a 77 GHz antenna (diameter: 90 mm, height: 22 mm), fed by three different feeds. The reflectarray substrate thickness was 0.254 mm, and the dielectric constant was 2.22; the polarizing slot array substrate thickness was 1.02 mm, and the dielectric constant was 4.5.

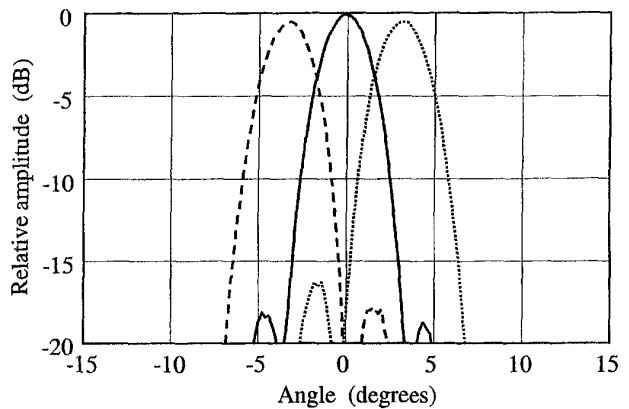


Figure 12b. Details of the scanning performance for the antenna of Figure 12a.

3.2 Multi-Beam Antennas

In a number of applications, and especially for automotive radar applications, some beam scanning is required. The folded reflector antennas, as described here, enabled a simple mechanical

beam scan by tilting only the reflectarray [8]. The feed and the mm-wave front-end, as well as the polarizer, remained fixed. The reflectarray itself was very lightweight; in addition, the resulting antenna beam was scanned at twice the angle of the reflectarray (Figure 9).

A 76.5 GHz antenna with a movable reflector was designed, fabricated, and tested. The antenna diameter was 100 mm, and the distance between the reflector and polarizer was 25 mm. For this antenna, a slot array on a substrate of 1.02 mm thickness with a dielectric constant of 4.5 was employed. This allowed good polarizer properties using a commercially available substrate material and thickness at this frequency, although a printed grid would have given slightly lower losses. In the test arrangement, the reflector angle was adjusted by a screw, and kept in place by a spring. In an actual application, a small motor or a simple magnetic mechanism could perform this task. Figure 10 shows the radiation patterns for an *H*-plane scan from -8° to $+8^\circ$. The beamwidth for the center beam was 2.7° . The sidelobe level was better than -20 dB, up to a scan angle of 6° . The gain of this antenna was measured to be 35 dB. By rotating the polarizer and the feed polarization by 90° , scanning in the *E* plane was achieved, and very similar radiation characteristics have been measured.

In many of the present automotive-radar systems, only three beams are used, based on three separate feeds [10-12]. This type of beam scanning can be performed equally well using an antenna such as described here (Figure 11). The *E*-plane radiation diagrams of a 77 GHz antenna with a diameter of 90 mm and a depth of 22 mm are presented in Figure 12. The beamwidths were 2.9° for the center beam, and 3° for the tilted beams. As the feed horn diameter had to be quite small to enable closely spaced beams, a relatively strong illumination of the reflector edges had to be accepted. Together with some coupling between the three feeds, this led to a slight increase in sidelobe level. The antenna properties remained nearly unchanged in the frequency range assigned to this application, from 76 to 77 GHz.

4. Conclusion

The application of printed quasi-periodic structures to the design of folded reflector antennas has been demonstrated. To this end, use was made of the dual-polarization properties of the printed structures, enabling a polarization twisting. The results of four different antennas have been presented. The folded reflector antennas show very good radiation characteristics, low losses, and a comparably low height. Consisting of two printed substrates only, these can be a promising alternative to conventional printed or slotted waveguide array antennas.

5. Acknowledgment

Part of this work was funded by the German Research Association (DFG).

6. References

1. R. Mittra et al., "Techniques for Analyzing Frequency Selective Surfaces - A Review," *Proceedings of the IEEE*, **76**, 12, December 1988, pp. 1593-1615.

2. W. Menzel, "A Planar Reflector Antenna," MIOP 1995, Sindelfingen, Germany, pp. 608-612.

3. D. M. Pozar, S. D. Targonski, and H. D. Syrigos, "Design of Millimeter Wave Microstrip Reflectarrays," *IEEE Transactions on Antennas and Propagation*, **AP-45**, 1997, pp. 287-296.

4. J. A. Encinar, "Design of a Dual Frequency Reflectarray using Microstrip Stacked Patches of Variable Size," *Electronic Letters*, **32**, June 1996, pp. 1049-1050.

5. J. Huang, "Microstrip Reflectarray," IEEE International Symposium on Antennas and Propagation *Digest Volume 2*, 1991, pp. 612-615.

6. R. D. Javor, X.-D. Wu, and K. Chang, "Design and Performance of a Microstrip Flat Reflectarray Antenna," *Microwave and Optical Technology Letters*, **7**, 7, 1994, pp. 322-324.

7. D. Pilz and W. Menzel, "Periodic and Quasi-Periodic Structures for Antenna Applications," *Proceedings of the 29th European Microwave Conference 1999, Volume III*, Munich, Germany, pp. 311-314.

8. W. Menzel, D. Pilz, and R. Leberer, "A 77 GHz FM/CW Radar Front-End with a Low-Profile, Low-Loss Printed Antenna," *IEEE Transactions on Microwave Theory and Techniques*, **MTT-47**, 12, December 1999, pp. 2237-2241.

9. W. Menzel and D. Pilz, "Printed Quasi-Optical mm-Wave Antennas," Millennium Conference on Antennas and Propagation AP2000, Davos, Switzerland, Session 3A2-1, Paper 0023.

10. H. H. Meinel, "Automotive Millimeter-Wave Radar," *Proceedings of the 28th European Microwave Conference, 1998, Volume 1*, Amsterdam, Netherlands, pp. 619-629.

11. H. Daembkes and J. F. Luy, "Millimetre-Wave Components and Systems for Automotive Applications," *Microw. Engineering Europe*, December/January 1996, pp. 43-48.

12. I. Gresham, N. Jain, T. Budka, A. Alexanian, N. Kinayman, B. Ziegner, S. Brown, and P. Staecker, "A 76-77 GHz Pulsed-Doppler Radar Module for Autonomous Cruise Control Applications," *IEEE Transactions on Microwave Theory and Techniques*, **MTT-49**, 1, January 2001, pp. 44-58.

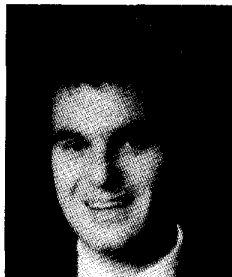
Introducing the Feature Article Authors



Wolfgang Menzel got his Dipl.-Ing. degree at the Technical University of Aachen, Germany, in 1974, and the Dr.-Ing. degree from the University of Duisburg, Germany, in 1977. From 1979 to 1989, he worked in the mm-wave department of AEG in Ulm, Germany (now European Aerospace, Defense, and Space Systems,

IEEE Antennas and Propagation Magazine, Vol. 44, No. 3, June 2002

EADS). From 1980 to 1985, he was head of the laboratory for integrated mm-wave circuits, and from 1985 to 1989, he was head of the complete mm-wave department. During that time, his areas of work included planar integrated circuits (mainly on the basis of finline techniques), planar antennas, and systems in the mm-wave frequency range. In 1989, he received a full Professorship at the University of Ulm. His current areas of interest are multi-layer planar circuits, waveguide filters and components, antennas, mm-wave and microwave interconnects and packaging, and mm-wave application and system aspects. From 1997 to 1999, he served as "Distinguished Microwave Lecturer," with the topic of "Microwave/Millimeter Wave Packaging." Dr. Menzel is a Fellow of the IEEE.



Dietmar Pilz got his Dipl.-Ing. degree from the University of Ulm, Germany, in 1994, and the Dr.-Ing. degree from the University of Ulm, Germany, in 1999. From 1994 to 1999, he worked in the Microwave Department of the University of Ulm as a Research Assistant and PhD student. His areas of work included planar and quasi-planar structures for antenna applications. In 1999, he joined DaimlerChrysler Aerospace in Ulm (now European Aerospace, Defense, and Space Systems, EADS). His current areas of interest are mm-wave circuits and systems, and antennas.



Maysoun Al-Tikriti got her bachelors degree from the University of Bagdad, Iraq, and her Dipl.-Ing. degree from the University of Paderborn, Germany. Since February, 2000, she has been working as a Research Assistant and PhD candidate in the Microwave Department of the University of Ulm, Germany. Her areas of work are planar and quasi-planar antennas, and reflectarrays. ☎



Editor's Comments *Continued from page 7*

reflects the other. The second structure is a printed reflectarray, formed by a periodic array of printed patches. The field from the feed strikes the polarization filter. One polarization is transmitted, while the other is reflected back to the reflectarray. The reflectarray is designed so that when it reflects the field back towards the polarization filter, there is a phase-angle shift and the field's

polarization is twisted. This permits the polarization to match that of the filter, so that field is transmitted through it. It also provides a sufficient degree of freedom that by varying the phase change across the reflectarray, the spherical wave originating from the feed is transformed into a plane wave as it leaves the polarizing filter. The resulting antenna thus involves only a waveguide feed and two closely spaced printed structures. The authors illustrate the advantages of the design with several prototypes, operating at frequencies of 61 GHz and 76.5 GHz.

In high-power microwave (HPM) applications, it is desirable to have an antenna that can accept an axially symmetric mode, and that can radiate with a peak in the pattern along the boresight of the antenna. This is not easily done, particularly with an antenna design that is appropriate for high-power applications. Clifton Courtney, Donald Voss, Carl Baum, William Prather, and Robert Torres describe a novel reflector-antenna design that accomplishes this in their feature article. The antenna works by varying the electrical path length from the feed to the aperture plane as a function of the azimuthal angle around the axis of the reflector. This is accomplished by segmenting the reflector's surface, and distorting it to produce a stepped surface for the reflector. The result is a circularly polarized radiated field with a boresight peak, in a design that works quite well at high power levels. Any desired linear polarization can also be achieved. The results of tests with several prototypes are presented, and a useable bandwidth of 60:1 was demonstrated for one of these.

Integral-equation techniques are widely used for the numerical solution of electromagnetic boundary-value problems. Typically, a problem is formulated in terms of a known excitation field, and unknown equivalent (continuous) electric and magnetic currents distributed over the boundary surface. The boundary conditions are expressed in terms of the known field and the unknown currents, and the unknowns are solved for – often using the Method of Moments, for example. In the Method of Auxiliary Sources (MAS), currents are not used. Instead, fictitious, equivalent point sources – the auxiliary sources – located near the boundaries, are used. These auxiliary sources are chosen such that their fields are elementary analytical solutions to the boundary-value problem. The fields on each side of the boundary are then expressed as weighted superpositions of these analytical solutions, and the unknown weights are solved for, using the boundary conditions. The feature article by Dimitra Kaklamani and Hristos Anastassiou reviews the MAS, presenting it in a particularly easy-to-understand fashion. The authors then discuss a key point in the application of the method: how best to choose the auxiliary sources. They review a variety of important recent developments related to the MAS, and describe a new, modified MAS. They also provide an interesting application of the MAS to the computation of the RCS of jet-engine inlets. They show that for comparable problems, the MAS can achieve a computational efficiency that is a factor of 10 greater than the MoM. I urge you to read this very understandable review: the tool described is potentially very important.

Our Other Contributions

Peter Staecker, our Division IV Director, continues his series of reports on the IEEE's fiscal state of affairs. He reports on the latest results from the June "organizational unit" meetings. It is finally beginning to appear that the IEEE is taking steps that might actually solve some of the long-term problems that led to the current financial crisis. In my opinion, we are very fortunate to have someone representing us who is so good about keeping us

Continued on page 64